3rd International Symposium on High-Temperature Metallurgical Processing
Edited by: Tao Jiang, Jiann-Yang Hwang, Patrick Masset, Onuralp Yucel, Rafael Padilla, and Guifeng Zhou
TMS (The Minerals, Metals & Materials Society), 2012

CHLORINATION OF TITANIA FEEDSTOCKS

Samantha Moodley[1], Rauf Hurman Eric[2], Cevat Kucukkaragoz[2], Aditya Kale[3]

[1]Exxaro Resources, Pretoria West, 0001, South Africa
[2]University of the Witwatersrand, Johannesburg, 2000, South Africa
[3]Mintek, Johannesburg, 2125, South Africa

Key words: Chlorination, Titania Feedstocks, Fluidization, Blowover

Abstract

Two titania slags, rutile and synthetic rutile were chlorinated with petroleum coke and CO in a small bubbling fluidized bed reactor. The study aims to identify differences in chlorination mechanism, compare conversion rates, blowover and the chlorination of impurities for the various titania feedstocks at different temperatures.

Chlorination rates were highest at 1000ºC; rutile chlorination significantly increases as temperature increases from 800ºC to 1000ºC. At 1000ºC, synthetic rutile had the highest chlorination conversion rate; this was followed by Slag B which in turn was more reactive than Slag A and rutile. The mechanism for slag, synthetic rutile (SR) and rutile chlorination differs. Synthetic rutile feed is porous, providing a larger surface area for the chlorination reaction, hence the highest conversion rates was attained. Titania slag becomes porous with the initial chlorination of FeO and MnO whilst rutile remains solid. As the porosity of slag particles increases so does its tendency to be elutriated. Ti_2O_3 is oxidized within the early stages of chlorination during the chlorination of FeO and MnO. Ti_2O_3 not oxidized is then rapidly chlorinated.

Introduction

Titanium dioxide (TiO_2) is the most common compound of titanium, about 95 - 98% of extracted titanium minerals is processed into TiO_2 white pigment [1]. Two processing routes exist for the production of TiO_2 pigments, i.e., sulphate and chloride based processes. In the chloride process, titania feedstock is fed to a fluidized bed reactor together with reductant and chlorine gas. A temperature of 1000 - 1300ºC is maintained in the reaction zone and apart from silica, zirconia, uranium and thorium, virtually all the metal oxides in the feed are converted to their respective chlorides [2]. Chlorine is recovered and recycled back to the reactor.

The feed to the chlorinator includes a number of titania feedstocks namely, synthetic rutile (SR), natural rutile, upgraded titania slag (UGS) and titania slag produced from ilmenite smelting. Natural rutile is the preferred feedstock for chlorination but due to dwindling reserves other titania feedstocks are substituted as feed for pigment production.

Fluidized bed technology is employed for the chlorination process, so feedstock physical characteristics such as density, size and shape factor is of importance. The feedstock has to have sufficient grain size and bulk density in order for the material to fluidize and to minimize

blowover carryovers from the chlorinator. A high elutriation rate translates to a shorter residence for particles in the fluidized bed which in turn negatively affects conversion efficiencies.

Since feedstock origin and production techniques differ, the physical properties and phase chemistry differ of the feedstocks will also differ, this will in turn impact the way in which each feedstock reacts in the chlorinator, although the TiO_2 content might be similar.

A number of studies have been completed on the chlorination kinetics of different feedstocks [3, 4, 5, 6, 7, 8]. Few studies have addressed the microstructural changes of titanium-bearing materials during the chlorination reaction [9, 10, 6]. Zhou et al., [9] studied the changes in ilmenite, SR, rutile, beneficiated slag and found that the rapid chlorination of easily chlorinated iron oxide in titania slag creates porosity that extends deeply into the interior of the particles. Nell and den Hoed [10] found that chlorination is associated with significant increases in particle porosity (even for rutile), which is brought about by the rapid initial chlorination of FeO and MnO (in ilmenite and slag) and (it is argued) by the chlorination of Ti_2O_3 which forms at high-energy surface sites.

This paper considers the chlorination of two slags, rutile and SR, the impact of elutriation on chlorination efficiencies and effects of Ti_2O_3 on chlorination.

Experimental Details

Samples - The test samples (i.e., Slag A, Slag B, rutile and SR) were subjected to carbochlorination experiments at temperatures ranging from 800ºC to 1000ºC in a fluidized bed reactor. Petroleum coke (i.e., 1.5 - 5mm, 97% Carbon) and CO gas was added as reductant. Slag A and rutile was acquired from South African producers whilst Slag B and SR were from international producers. In order to minimize the effect of size on chlorination rate, a common size range was selected for the experiments (i.e., 106 - 300µm). Den Hoed and Nell [10] found that at carbon levels lower than 15wt%, availability of carbon was the rate limiting step but once the stoichiometric requirement is exceeded the reaction proceeds unhindered. In this experimental procedure, 17wt% coke was added to the feedstock.

Apparatus - The chlorination experiments were conducted in an externally heated quartz reactor (80mm in diameter and 1100 mm in length). A porous distributor plate supported the charge and allowed for the even distribution of fluidizing and chlorination gases. Bed temperature was measured with a K type thermocouple. The crossover duct allows for the passage of the product gases and elutriated particles from the quartz reactor into the gas system. The crossover duct is connected to a condenser. High boiling point metal chlorides are condensed in the condenser and uncondensed gases are vented off to the caustic scrubber. Gas velocity is reduced in the round bottom flask and blowover settles out here. Figure 1 is an illustration of the experimental set up.

Procedure - The charge (i.e., 200g feedstock and 40g petroleum coke) was fluidized with argon during the heat up. Approximately 2% of the feed was elutriated during the heat up; this amount was considered insignificant in comparison to the feed mass. When the bed temperature reached the desired experiment temperature, the argon gas was switched off and a CO and Cl_2 mixture was fed to reactor. Gas flow (i.e., Cl_2, CO) was controlled by rotameters to give a superficial gas velocity of 39.8cm/s. The flow rates of Cl_2 and CO gas were maintained at 8Nl/min and 4Nl/min respectively. The total gas pressure inside the fluid bed reactor was approximately 85kPa, the

partial pressure of Cl_2 gas in the fluid bed reactor was approximately 57kPa. Upon completion of the test, the blowover and bed residue was collected. The large carbon particles were screened out of the bed sample. The blowover and bed sample was washed with water and dried at 105°C for 2 hours. Thereafter the material was roasted at 900°C for 2 hours to burn off fine coke particles.

Analytical Techniques - The chemical analysis of feed material and chlorinated bed samples were determined by Inductively Coupled Plasma Optical Emission Spectrometry (ICP – OES) techniques, particle size by screening and density by helium pycnometry. X-Ray diffraction (XRD) and Scanning Electron Microscope (SEM) were used for mineralogical characterization of the feed and the chlorinated bed samples, equipment and software details are described elsewhere [11].

Using the masses of the feed, bed residue and blowover, the conversion to gaseous chlorides was calculated as follows:

$$Conversion(\%) = \frac{M_i - (M_E + M_B)}{M_i} \quad (1)$$

M_i is the initial mass of sample charged to reactor, M_e is the mass elutriated from the reactor and M_b is the mass of sample remaining in the reactor at the end of the experiment. The degree of conversion is affected by kinetics of the reaction as well physical properties of feedstock since blowover is considered.

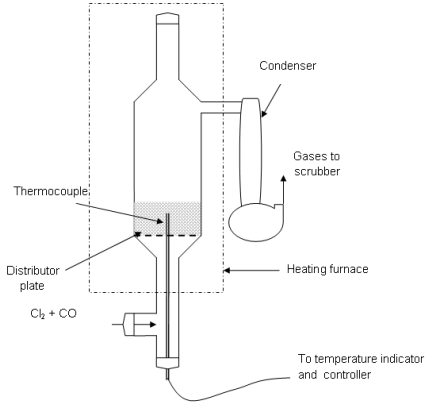

Figure 1: Schematic of Experimental Set up for Chlorination Experiments

Results and Discussion

Sample Characterization

Feedstock chemical composition is reported in Table I.

Table I: Feedstock Chemical Composition, Average Particle Size and Density

	Slag A	Slag B	Rutile	SR
SiO_2 (wt%)	1.64	1.49	1.44	0.80
Al_2O_3 (wt%)	1.02	1.64	0.31	1.80
FeO (wt%)	8.60	1.96	0.49	3.43
Fe (metallic) (wt%)	0.00	1.03	0.00	0.10
TiO_2 (equivalent)*(wt%)	87.46	95.02	95.69	92.77
Ti_2O_3 (wt%)	23.42	38.80	0.00	10.30
TiO_2 (wt%)	61.92	51.90	95.69	81.40
CaO (wt%)	0.22	0.26	0.08	0.10
MgO (wt%)	0.73	0.25	0.01	0.31
MnO (wt%)	1.90	2.80	0.01	1.00
Impurities† (wt%)	1.11	0.73	1.52	0.76
d_{50} (µm) of feed	294	218	110	151
Average density(kg/m^3)	4025	4033	4172	4254

*** Ti^{3+} and Ti^{4+} expressed as TiO_2, † sum of Na_2O, Nb_2O_5, K_2O, Cr_2O_3, V_2O_5, P_2O_5, ZrO_2**

The slags are products of ilmenite smelting and as a result of the milling process is more brittle, angular and irregularly shaped than rutile and SR. Slag A and B has a wider particle size distribution than rutile and SR. The difference in the shape and size is evident from the scanning electron microscope (SEM) back scattered electron (BSE) images, Figure 2.

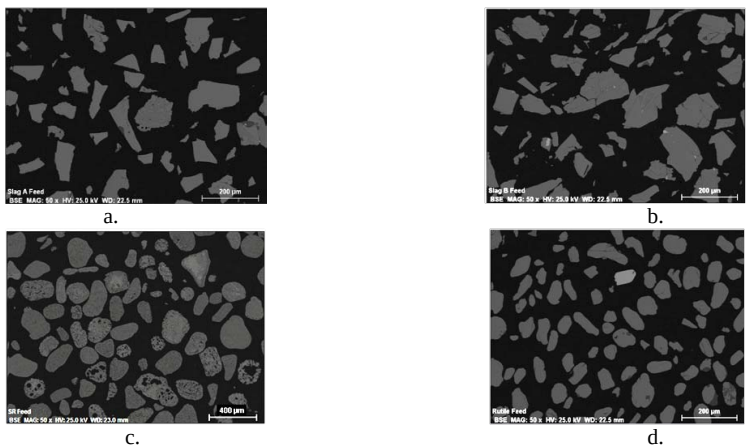

a. b. c. d.

Figure 2: BSE Images of a Section through a. Slag A, b. Slag B, c. SR, d. Rutile

There are four phases (i.e., solid solution, rutile, metallic iron and glassy) present in high titania slags [12]. The major phase is a solid solution referred to as the M_3O_5 phase. This phase is a solid solution of the end members $FeTi_2O_5$, Ti_3O_5, $MnTi_2O_5$, $MgTi_2O_5$, Cr_2TiO_5, Al_2TiO_5 and V_2TiO_5 [13]. The glassy phase was present in various shapes and sizes throughout most of the Slag A and Slag B particles. The glassy phase consists of mainly of SiO_2, with smaller amounts of Al_2O_3 and TiO_2. Tabular lath like rutile crystals with fine grained metallic iron precipitates was found in Slag A. Bessinger [14] and Toromanoff and Habashi [15] also found metallic iron to be present in the rutile phase in the slag.

The iron present in Slag A is between 1 and 2 μm whereas in Slag B it is approximately 20μm and associated with carbon. The chemistry and size of the iron droplets suggest that the iron was trapped in a viscous slag and did not precipitate during cooling as with Slag A. A magnified Slag A particle showing the various phases is presented in Figure 3a. In the magnified particle, the dark grey phase is the silicate/glassy phase, the light grey is the M_3O_5 phase, the bright spots are the Fe and the intermediate grey bands are the rutile.

The SR sample is a product of the acid leaching process. The leaching of the iron fraction leaves behind a porous particle with TiO_2 content above 90%. The sample contained a few particles that appear to have escaped the leaching process with iron fraction still present. A porous particle and iron containing particle is shown alongside each other in Figure 3b. The rutile sample primarily consists of unaltered rutile particles with a few zircon grains.

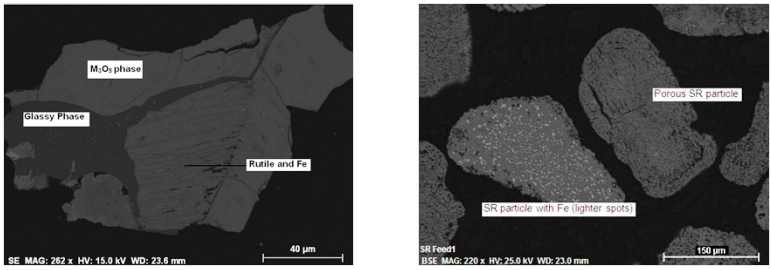

a. b.

Figure 3: BSE Image of a Section through a. Slag A Feed and b. SR Feed

Chlorination Results

Effect of Temperature - Slag A, Slag B and rutile were chlorinated at 800, 900 and 1000°C with coke and CO. Results are presented in Figure 4 and 5, the conversion (%) is calculated using Equation 1. Temperature had a significant effect on the overall conversion rate with the chlorination of rutile especially hindered at lower temperatures. Slag B shows the highest degree of conversion, with Slag A following closely behind. At 800°C, only 15% of rutile is chlorinated compared to 60% at 1000°C. It is clear to see why the commercial chlorination process is carried out at temperatures of 1000°C and higher. Iron chlorination in Slag A and Slag B is complete at 800°C. MnO chlorination in rutile is complete at 800°C, MnO chlorination in the slags improves slightly with increasing temperature. The chlorination of Al_2O_3 to $AlCl_3$ significantly improves

with increasing temperature; there is a 40% improvement in Al_2O_3 chlorination when the temperature is increased from 800°C to 1000°C. MgO chlorination in the Slag A and Slag B improves with increasing temperature. Complete MgO chlorination is achieved in the rutile sample at 800°C. The mass balance indicates that there is more SiO_2 in the bed sample than at the start of the reaction; this difference is approximately 1g to 2g and is considered insignificant compared to the total sample mass. This is likely due to analytical error. However, this indicates that SiO_2 does not chlorinate significantly during the experiment.

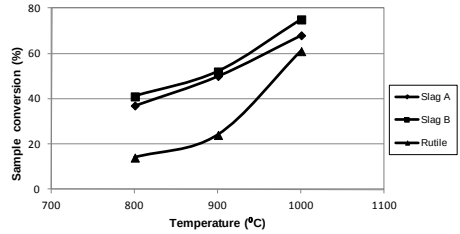

Figure 4: Chlorination of Three Feedstocks for 3 hours

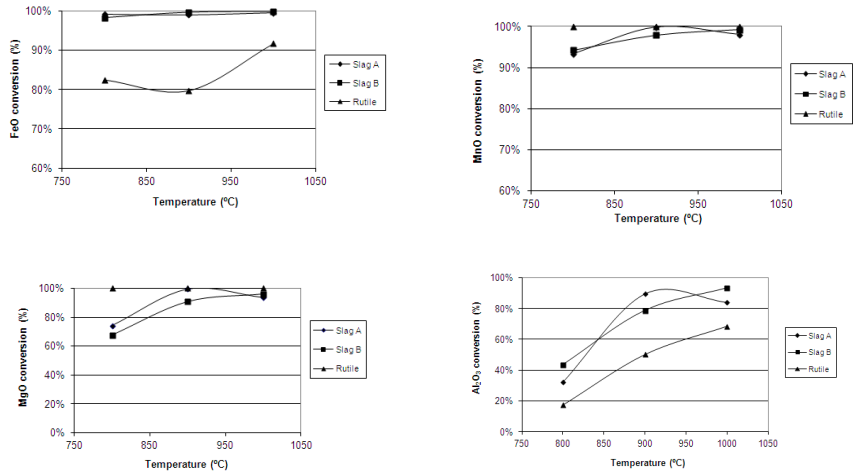

Figure 5: Chlorination of FeO, MnO, Al_2O_3 and MgO for 3 hours

Effect of Time - The conversion results from the chlorination experiments conducted at 1000°C is shown in Figure 6, the blowover and bed residue is given in Table II. After 3 hours of chlorination, the highest degree of conversion was achieved with the SR sample; this was followed by Slag B, Slag A and rutile. Slag A and rutile blowover increased with increasing

reaction time. Although the conversion of Slag A and SR differ by 23% after 3 hours of chlorination, the remaining bed sample after the experiment was similar. The difference in conversion results was due to the blowover, a significant amount of partially reacted Slag A particles was elutriated after 3 hours whereas blowover from the SR experiment was low. Blowover decreases chlorinator efficiency and this effect is illustrated with Slag A where degree of conversion of Slag A was lowered because 53g of partially reacted feedstock was blown out of the reactor during the 180 minute experiment.

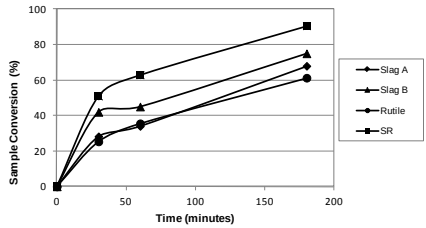

Figure 6: Conversion of Slag A, Slag B, SR and Rutile at 1000°C

Table II: Blowover and Remaining Bed Mass of Slag A, Slag B, SR and Rutile after Chlorination at 1000°C for Different Times

Feedstock	Blowover (g)			Remaining Bed Sample (g)		
	30 (minutes)	60 (minutes)	180 (minutes)	30 (minutes)	60 (minutes)	180 (minutes)
Slag A	2	7	53	142	125	11
Slag B	4	2	3	112	108	48
Rutile	0	1	30	149	128	47
SR	0	1	1	98	71	18

Chlorination Mechanism - The remaining bed samples after the 30, 60 and 180 minute experiments at 1000ºC were collected and prepared for SEM analysis. BSE images of the 1000ºC, 30 minute experiments are presented in Figure 7. The BSE images together with chemical analysis and EDS analysis provided vital information towards identifying and understanding the difference in the chlorination mechanism between the feedstocks. With the exception of samples that were chlorinated for 1 minute, rutile was identified as the major titania phase in all the bed samples. A study of the surface of the bed samples after 30 minutes of chlorination shows different levels of porosity between Slag A, Slag B and SR samples.

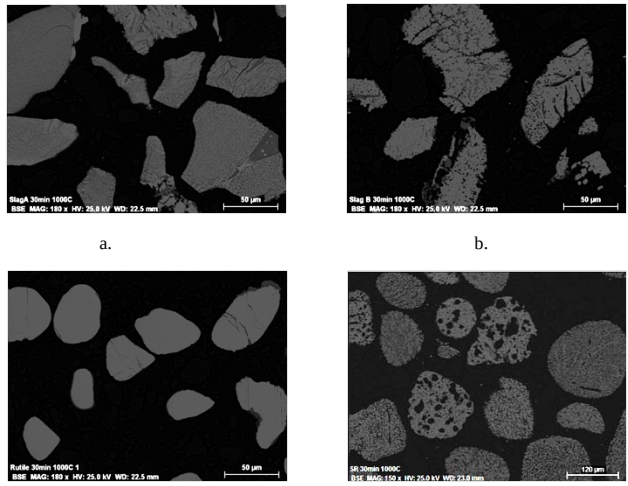

a. b.

c. d.

Figure 7: BSE Images of a Section through a. Slag A, b. Slag B, c. Rutile, d. SR after 30 minutes of Chlorination at 1000°C

Slag A and Slag B - BSE images of Slag A after 1 minute of chlorination at 1000°C is shown in Figure 8. The chemical analysis of the bed samples indicates that 80% of FeO and 63% MnO was chlorinated during the first minute of the experiment. The chlorination of Fe and Mn leaves behind porous particles with a large surface area for subsequent reaction. Small amounts of Cl_2 were identified on the boundary of the pores. The presence of chlorine around the pores indicates that the reactive gases diffused into the slag particle and chlorination was not restricted to the outer surface. Pore size increases with increasing chlorination duration and the particles become lighter and can be elutriated from the reactor. This is evident with Slag A as blowover increased from 7g to 50g after 60 and 180 minutes of chlorination. Silica removal was many times slower than TiO_2 chlorination; unreacted free-lying silicate pieces collected in the bed after the chlorination of the rest of the particle that it was initially apart of.

Slag B (i.e., the higher TiO_2 content slag) feed was brittle and contained more cracks than Slag A. Due to the lower iron content; the porosity was not as widespread as in Slag A after 30 minutes of chlorination. However the larger Fe droplets in Slag B feed left behind larger pores upon chlorination. Chlorine attack widens the cracks causing particle breakage; the smaller pieces of slag are then converted to gaseous metal chloride before the particle is elutriated.

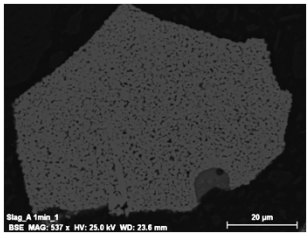

Figure 8: BSE Image of a Section through Slag A after 1 minute of chlorination at 1000°C

Rutile - After 30 minutes of chlorination, the rutile particles are dense and smooth show no signs of porosity. Rutile particles grow smaller as chlorination proceeds according to a shrinking core mechanism.

Synthetic rutile - SR feed particles are porous so the surface area available for chlorination was large from the start. After 30 minutes of chlorination, the initial pores left behind by the leaching of the iron have grown into larger pits. The SR particles are rapidly chlorinated before they are elutriated.

Effect of Ti_2O_3 - During ilmenite smelting, some TiO_2 is reduced to Ti_2O_3 according to reaction 3.

$$2\ TiO_2 + C = Ti_2O_3 + CO \qquad (3)$$

Ti_2O_3 is not desired as it does not increase the equivalent TiO_2 content of slag but consumes more electrical energy and carbon [16]. Le Roux [6] chlorinated slag in the absence of reductant (i.e., no coke and/or CO) and found that chlorination reactions still took place albeit to a lesser extent. It was demonstrated by mass balance methods that there was sufficient Ti_2O_3 to act as reductant for the chlorination of FeO and MnO. The remaining Ti_2O_3 was rapidly chlorinated.

In this study, experiments were conducted with CO and coke; so thermodynamic calculations were done to determine whether chlorination with coke, CO, or Ti_2O_3 would be more thermodynamically feasible. Using Factsage Version 6.1, a thermodynamic software tool, the change in Gibbs free energy at 1000ºC for Reactions 4 to 9 was determined. The change in Gibbs free energy is negative for all six reactions; however reaction with Ti_2O_3 for both FeO and MnO chlorination is more negative indicating that these reactions are more thermodynamically favorable.

$$MnO + Ti_2O_3 + Cl_2 \rightarrow MnCl_2 + 2TiO_2 \qquad (\Delta G = -277\ kJ/mol\ MnO) \qquad (4)$$

$$MnO + CO + Cl_2 \rightarrow MnCl_2 + CO_2 \qquad (\Delta G = -191\ kJ/mol\ MnO) \qquad (5)$$

$$MnO + C + Cl_2 \rightarrow MnCl_2 + CO \qquad (\Delta G = -243\ kJ/mol\ MnO) \qquad (6)$$

$$FeO + Ti_2O_3 + Cl_2 \rightarrow FeCl_2 + 2TiO_2 \qquad (\Delta G = -273\ kJ/mol\ FeO) \qquad (7)$$

$$FeO + CO + Cl_2 \rightarrow FeCl_2 + CO_2 \qquad (\Delta G = -187\ kJ/mol\ FeO) \qquad (8)$$

$$FeO + C + Cl_2 \rightarrow FeCl_2 + CO \qquad (\Delta G = -239\ kJ/mol\ FeO) \qquad (9)$$

Slag A was chlorinated for 1 minute at 1000ºC with petroleum coke (17wt% of charge) to determine the effect of Ti_2O_3 on chlorination. The mass balance is presented in Table III. After 1 minute of chlorination, 5g of Ti^{3+} was chlorinated and 74% of Ti^{3+} oxidized to Ti^{4+}. According to stoichiometry there was sufficient Ti_2O_3 to act as reductant for the chlorination of MnO and FeO.

Table III: Slag A Mass Balance After 1 minute of Chlorination at 1000 ºC

Elements	Feed Material		Bed Sample		Mass chlorinated (g)	Conversion (%)
	Analysis (%)	Mass (g)	Analysis (%)	Mass (g)		
Ti (tot)	52.42	104.83	55.90	99.89	4.94	5%
Ti^{3+}	15.51	31.02	1.89	3.38	27.64	
Ti^{4+}	36.91	73.81	53.98	96.46		
FeO	8.60	17.20	1.89	3.38	13.82	80%
MnO	1.90	3.80	0.78	1.39	2.41	63%

The result of the 1 minute experiment has shed some light on the difference between the TiO_2 chlorination rate of Slag A and Slag B (Figure 9). TiO_2 chlorination in Slag A after 30 minutes of chlorination at is only 20% after 30 minutes, whereas chlorination in Slag B is 41%, the difference is likely due to the Ti_2O_3 content of the slag's, Slag B has 39 % whereas Slag A has 23%. The results of the 1 minute chlorination experiment show that Ti_2O_3 not oxidised in the chlorination of FeO and MnO is then rapidly chlorinated, since Slag A has a higher FeO content compared to Slag B (i.e., 9 % vs 2 %) there is less Ti_2O_3 available for chlorination, in addition Slag B had a higher Ti_2O_3 content to start with. This provides an explanation as to why chlorination in Slag B was higher than Slag A.

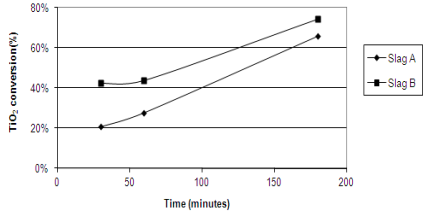

Figure 9: TiO_2 Conversion of Slag A and Slag B at 1000ºC

Although rutile and Slag B feed have approximately the same $TiO_{2\ (equivalent)}$ content (i.e., 95%), overall conversion of rutile after 180 minutes is 14% lower than Slag B. This is likely due to combination of the effects of rapid chlorination of the Ti_2O_3 fraction in Slag B and the Fe content in Slag B which leaves behind a porous matrix and larger surface area for subsequent chlorination.

Conclusion

Chlorination rate increases with increasing temperature and the chlorination of rutile is most affected by lower temperatures. At 1000ºC, SR had the highest chlorination conversion rate; this was followed by Slag B which in turn was more reactive than Slag A and rutile.

SR feed is porous; this allows for easy diffusion of reactive gases and chlorination proceeds quickly. The rapid chlorination of iron from slag leaves behind a porous high titania matrix with a large surface area for subsequent reaction. In this process, the density of the slag is lowered and it can be elutriated from the reactor. Rutile chlorination proceeds along the surface of the particle; so particle size decreases with increasing chlorination time.

Ti_2O_3 acts as reductant for the chlorination of FeO and MnO, Ti_2O_3 not oxidized is rapidly chlorinated.

Acknowledgements

Exxaro is acknowledged for permission to publish this paper. Appreciation is also expressed to Annabe Walliser and Jill Richards for SEM and XRD work.

References

1. H. Kotze, D. Bessinger, and J. Beukes, “Ilmenite Smelting at Ticor SA”, South African Pyrometallurgy Conference, Cradle of Human Kind, South African Institute of Mining and Metallurgy, (2006), 203 – 214
2. T.P. Battle, D. Nguyen, and J.W. Reeves, “The Processing of Titanium-containing ores”, The Paul E. Queneau International Conference, Extractive Metallurgy of Copper, Nickel and Cobalt, The Minerals, Metals and Materials Society, (1993), 925- 943
3. Y.K. Rao, and B.K Chadwick, “Chlorination of Rutile (TiO_2) with CO – Cl_2 – He gas mixtures”, Trans. Instn Min. Metall, 97, (1988), 167 – 179
4. A. J. Morris, and F. Jensen, “Fluidized Bed Chlorination Rates of Australian Rutile”, Metallurgical Transactions B, (1976), 89 – 93
5. W.E. Dunn, “High temperature chlorination of TiO_2 Bearing Minerals”, Trans AIME, 218, (1960), 6 – 12
6. J.T. Le Roux, “Fluidized bed chlorination of Titania slag” (MSc, University of Pretoria, 2001)
7. H.Y. Sohn and L. Zhou, “The Kinetics of Carbochlorination of Titania slag”, Canadian Journal of Chemical Engineering, 76, (1998), 1078 – 1082
8. H.Y. Sohn, L. Zhou, and K. Cho, “Intrinsic Kinetics and Mechanism of Rutile Chlorination by CO and Cl_2 Mixtures”, Ind. Eng. Chem. Research, 37, (1998), 3800 – 3805
9. L. Sohn, Y.H. Sohn, G.K. Whiting, and K. Leary, “Microstructural Changes in Several Titaniferous materials”, I & EC Research, 35, (1996), 954 – 962
10. J. Nell and P. Den Hoed, “The Carbochlorination of Rutile, Titania Slag and Ilmenite in a Bubbling Fluidized-bed Reactor”, XXII International Mineral Processing Congress, Cape Town, (2003), 133 – 143

11. S. Moodley, “A Study of the Chlorination Behaviour of Various Titania Feedstocks” (MSc thesis, University of the Witwatersrand, 2011)
12. D. Bessinger, H. Du Plooy, P.C. Pistorius, and C. Visser, “Characteristics of Some High Titania Slag”, Heavy Minerals Conference, Johannesburg, South Institute of Mining and Metallurgy, (1997), 151 – 156
13. H. Kotze, “Investigation into the Effect of Cooling Conditions on the Particle Size Distribution of Titania Slag” (PhD thesis, University of Pretoria, 2007)
14. D. Bessinger, “Cooling Characteristics of High Titania Slag” (MSc thesis, University of Pretoria, 2007)
15. I. Toromanoff, and F. Habashi, “The Composition of a Titanium Slag from Sorel”, Journal of the Less common metals, 97, (1984), 317 – 329
16. P.C. Pistorius, “The Relationship Between FeO and Ti_2O_3 in Ilmenite Smelter Slags” Scandinavian Journal of Metallurgy, (2001), 120 – 125